6 Messenger RNA expression profile analysis of *S.* Typhimurium infected esDCs

6.1 Introduction

6.1.1 *Salmonella*-DC interactions

S. Typhimurium is a food-borne pathogen that causes gastroenteritis in humans. After the bacteria have survived the acidic milieu of the stomach, they compete with the intestinal flora, cross the intestinal mucus layer and contact the gut epithelium cells, eventually penetrating the intestinal mucosa (Giannella *et al.*, 1972). It is believed that *Salmonella* preferentially invade the gut epithelium through M cells, which are specialized cells that lack the overlying mucus glycocalyx, making them more readily accessible to penetration by intestinal microbes (Gebert, 1997; Jepson & Clark, 2001; Neutra *et al.*, 2001). The underlying lamina propria is rich in DCs and macrophages poised to initiate and activate the immune response to pathogens. In this location, DCs can also inadvertently play an active role in facilitating the penetration of pathogenic bacteria through the gut epithelium barrier (Chieppa *et al.*, 2006; Rescigno *et al.*, 2001; Vallon-Eberhard *et al.*, 2006). DCs can extend cellular protrusion between epithelium cells and sample the lumen content, a process known as diapodesis. DCs express tight junction proteins that are able to open the tight junctions present between epithelial cells and sample the gut lumen while still preserving the integrity of the epithelial barrier. The DCs' ability to take up antigens, process and present them to naïve T cells on MHC molecules makes them indispensable for raising a specific and efficient immune response to invading pathogens.

DCs are key immune cells that are able to move around within the body and locate themselves in strategic sites anywhere pathogens are likely to attack the body, such as in the intestine. In the gut, DCs can be found in the lamina propria, in Peyer's patches, in the subepithelial dome, and beneath the follicle epithelium. *Salmonella* can be internalized by DCs resident in the subepithelial dome of Peyer's patches (Hopkins *et al.*, 2000) and infected DCs can serve as an alternative invasion route contributing to the

spread of bacteria inside the host (Cheminay *et al.*, 2002). Invading *Salmonella* are able to survive inside DCs without replicating, suggesting that this persistence is potentially the foundation of the development of the adaptative immune response to live *Salmonella*. This process could partially explain the systemic proliferation of bacteria even after a long period after infection and might be a requirement for the development of the carrier state. The persistence of *Salmonella* inside DCs appears to be associated with the ability of the bacteria to interfere with the MHC class II dependent antigen presentation through the activity of the SPI-2 system (Cheminay *et al.*, 2002; Jantsch *et al.*, 2003). The TIIISS encoded on SPI-2 can interfere with lysosomal fusion with the SCV (Uchiya *et al.*, 1999) and can promote the formation of the F-actin filament network around the SCV which is necessary for bacterial survival inside the vacuole (Meresse *et al.*, 2001).

The interaction between *S.* Typhimurium and DC has been the subject of a good deal of research since the first DCs were discovered in 1973. The importance of understanding the *Salmonella* interactions with the host may help to develop new more effective vaccines. Due to the emergence of multi-drug resistant strains (Cooke & Wain, 2006; Mirza *et al.*, 1996), *Salmonella* infections are occurring more frequently and are more difficult to cure.

6.1.2 Microarray analysis on DCs

Dendritic cells are versatile cells involved in the initiation of both innate and adaptive immunity. They are involved in the differentiation of regulatory T reg cells required for the preservation of self-tolerance. The plasticity of these cells has fascinated researchers for years and now it is possible to investigate aspects of the complete genetic reprogramming that these cells undergo in response to external stimuli using a microarray platform (Foti *et al.*, 2007). DCs can be stimulated to different degrees by various impulses and consequently it is possible to distinguish semi-mature DCs and fully-mature DCs. The semi-mature state is induced by two cytokines, TNFα and IL-4 (Granucci *et al.*, 2001; Menges *et al.*, 2002; Terme *et al.*, 2004). Full DC maturation is induced by microbial products, pathogen associated molecular patterns (PAMP) that bind to TLRs or toxins, and prostaglandins (Ausiello *et al.*, 2002; Hayashi *et al.*, 2001;

Poltorak *et al.*, 1998). However, our understanding of the biology of DCs is still advancing and we still have much to learn about mature and immature states.

In the last few years there has been an increased use of microarray analysis to investigate the nature of human and mouse DCs in order to unravel the mechanisms by which this complicated cell is regulated during infection (de Jong *et al.*, 2002; Jayakumar *et al.*, 2008; Konopka *et al.*, 2007; Lupo *et al.*, 2008; Yam *et al.*, 2008). Similar studies have also been directed at understanding the maturation process (de Jong *et al.*, 2002; de Jong *et al.*, 2005; Granucci *et al.*, 2001; Shin *et al.*, 2008). Microarray technology has proven to be a powerful tool to apply in this analysis.

The activation of the splenic DC line D1 by LPS and TNFα was investigated by microarray analysis by Granucci (2001) using GeneChip oligonucleotide probe arrays representing approximately 6,500 distinct mouse genes and ESTs (expressed sequence tags). They reported in total 59 'interesting' genes, among which cyclins and anti-proliferative genes were up-regulated during LPS treatment suggesting a definitive growth arrest and full cell maturation. Growth arrest is important to permit mature DCs to migrate into lymph nodes and prime CD8+ and CD4+ T cells. DCs activated with LPS also up-regulated IL-12p40, IL-1β and IL-6 in addition to the down-regulation of MHC class II, a further sign of cell maturation (Granucci *et al.*, 2001). This type of research can potentially lead to the identification of weaknesses in the host response and strategies employed by 'smart' pathogens. In this sense, very interesting work was carried out on *M. tuberculosis*, monitoring the interaction of this pathogen with macrophages and dendritic cells. In this study the researchers highlight some of the key pathways potentially involved in host-pathogen 'cross talk' (Tailleux *et al.*, 2008).

In addition to improving the understanding of natural events that occur in cell systems, microarrays can be used in applied research. Transcription profiling can assist in understanding how viral vaccine vectors trigger immune responses to chronic infections by studying the interaction between myeloid cells and vaccine vectors (Harenberg *et al.*, 2008). This research may reveal new mechanisms that lead to the activation of specific immune responses to target pathogens or cancer cells, information that may translate into effective vaccines or other immune therapies.

This chapter describes the results of transcriptome and FACS analysis looking at the esDC reaction to infection with *S.* Typhimurium.

6.2 Experimental design

Murine AB2.2 ES cells were driven to differentiation into esDCs in three independent experiments. After characterization by FACS the esDCs were infected with *S.* Typhimurium(p1C/1) expressing the GFP protein with the aim of FACS sorting infected from uninfected cells. Total RNA was extracted from nine samples: three samples were from sorted uninfected esDCs, three samples were from sorted infected esDC at 2 hours post-infection and three samples were from sorted infected esDCs at 4 hours post-infection. Relative amounts of cRNAs were hybridized onto whole genome Illumina MouseWG v1.1 arrays. The expression data were analyzed initially using the Bioconductor package and subsequently the InnateDB (Lynn *et al.*, 2008) platform was used to investigate cellular pathways that were significantly affected during infection.

.

6.3 Results

6.3.1 Infection of esDCs by *S.* Typhimurium SL1344

EsDCs infected with *S.* Typhimurium SL1344(p1C/1) expressing GFP were investigated by FACS analysis. EsDCs were collected and seeded at $2x10^5$ cells per well in 24 well plates and incubated overnight in medium without GM-CSF or IL-3. The cells were then infected at a MOI of 100. After 30 min incubation they were washed with warm PBS Ca^-Mg^- and incubated for 2, 4 and 6 hours with complete media containg 50µg/ml of gentamicin. Then they were washed and treated with a non-enzymatic cell dissociation buffer. Before FACS analysis the cells were fixed with 1% paraformaldehyde. The results of a typical infection are presented in Figure 6.1.

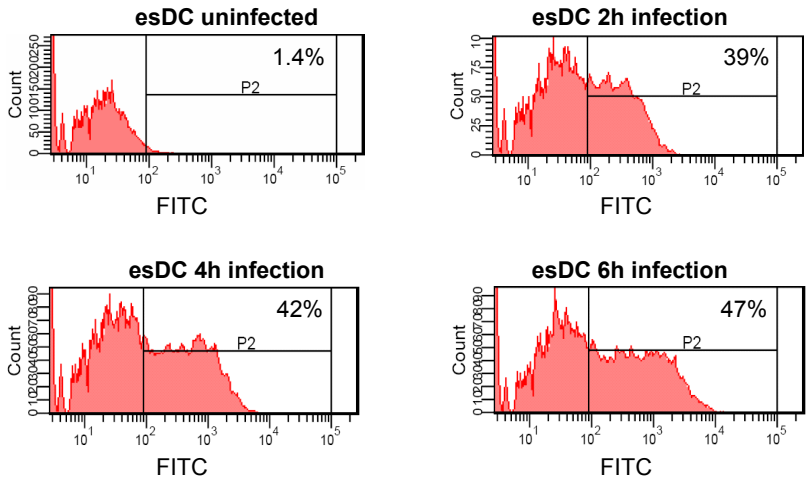

Figure 6.1 FACS analysis of esDCs infected with *S.* Typhimurium SL1344(p1C/1)

The esDCs were infected with *S.* Typhimurium(p1C/1) expressing GFP at MOI 100. The green bacteria were revealed by FACS and recorded in the FITC channel. Here, the results are reported from three time points of infection.

6.3.2 FACS sorting of esDCs infected with *S.* Typhimurium(p1C/1)

Three independent differentiation runs, performed on three independent AB2.2 murine ES cell cultures obtained from three different frozen stocks were infected with *S.* Typhimuriunm SL1344(p1C/1). The esDCs were sorted in order to collect the infected cells and extract total RNA to perform transcription analysis.

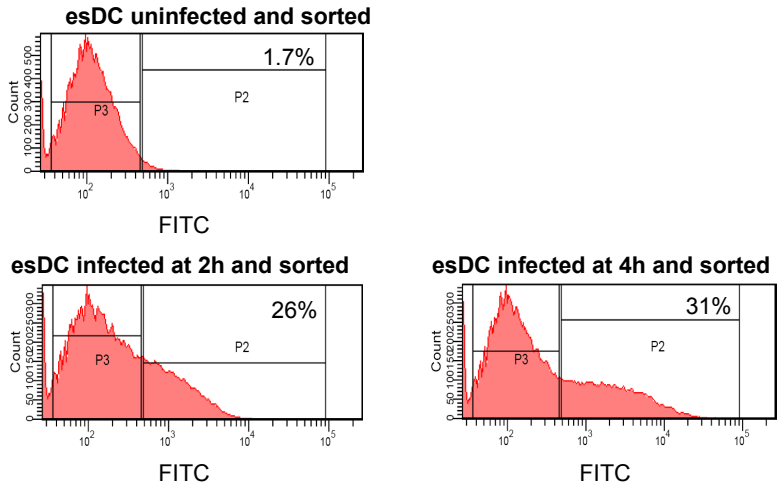

Figure 6.2 EsDCs were infected with *S.* Typhimurium SL1344(p1C/1) and FACS sorted for transcriptome analysis

This figure shows the second biological replicate of infected esDCs sorted in order to perform transcription profiling during *S.* Typhimurium infection. After excluding the debris, the cells were divided into two populations P3 (uninfected), and P2 (infected, positive for FITC) and these were sorted into two 15ml Falcon tubes containing 2ml of RNA ladder buffer. The sorting was carried out using a FACS Aria Cell-Sorting System with sorting mask 16-16-0 which defines the yield, the purity and the phase mask respectively. This sorting mask is suggested by the manufacture as optimal for two-way sorting.

6.3.3 Total RNA extraction, quantification and quality assessment

EsDCs were fully characterized for surface marker expression two days before infection. Total RNA from infected esDCs was extracted immediately after sorting. RNA quantification and quality analysis were carried out prior to storage at -80ºC. The total RNA was extracted using QIAGEN Mini Kit and after quantification using NanoDrop 1000 (Thermo) (Table 6.1), the RNA quality was tested by Bioanalyzer analysis (Figure 6.3).

Table 6.1 Total RNA concentration from esDC uninfected and infected with *S.* Typhimurium SL1344(p1C/1)

This table shows the efficiency of the sorting process and the amount of RNA extracted from each sorted population of cells used for microarray hybridization. N/A = not available.

ID	esDC	Status	Number of cells sorted	RNA quantity ng/µl	260/280
1B	1st biol rep	uninfected	1,874,218	222.98	2.02
2B	1st biol rep	infected 2h	753,621	59.85	2.06
4B	1st biol rep	infected 4 h	978,863	93.84	2.04
1E	2nd biol rep	uninfected	2,007,081	164.45	2.06
2E	2nd biol rep	infected 2h	754,809	55.45	1.97
4E	2nd biol rep	infected 4 h	1,054,440	59.94	1.95
1G	3rd biol rep	uninfected	N/A	82.67	2.08
2G	3rd biol rep	infected 2h	655,284	36.13	2.00
4G	3rd biol rep	infected 4 h	714,970	41.74	2.00

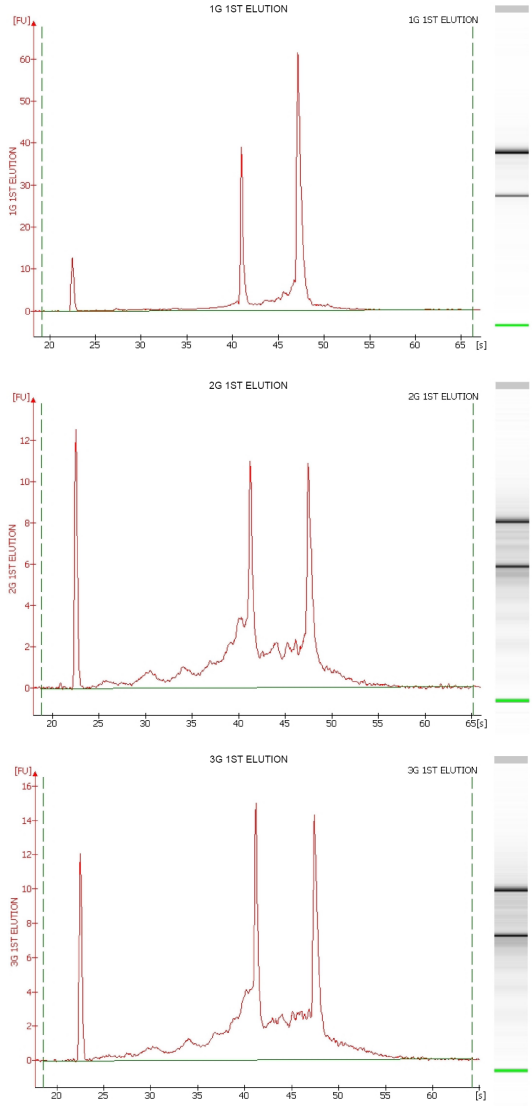

Figure 6.3 Bioanalyzer profile of the total RNA quality extracted from esDCs uninfected and infected with *S.* Typhimurium SL1344(p1C/1) at 2h and 4h

Three electropherograms from Bioanalyze analysis of total RNA extracted from esDCs uninfected and sorted (top histogram) and infected with *S.* Typhimurium at 2h (middle histogram) and at 4h (bottom histogram). The cells were sorted at the FACSAria Cell-Sorter System in 2ml of RNA ladder solution that preserves the RNA. Some degradation in the total RNA can be seen especially in the sample extracted from infected esDCs. However the two peaks corresponding to ribosome RNA 18S and 28S it can be still observed and their ratio is about 1:2.

6.3.4 cRNA synthesis, labeling and hybridization on Illumina arrays

The cRNA synthesis was performed by Peter Ellis working at the microarray facility at the WTSI following the manufacturer's instruction. Briefly 300ng of total RNA were employed to synthesize double stranded cDNA which was used to produce biotinylated antisense RNA (cRNA) using the Illumina TotalPrep-96 RNA Amplification Kit. The labelled cRNA was hybridized onto the MouseWG-6 v1.1 BeadChips at 58ºC overnight. Probe summaries were calculated prior to normalisation and analysis using BeadStudio.

6.3.5 Bioconductor analysis and pathway analysis with InnateDB

Bioconductor analysis was performed with Dr. Robert Andrew from the Microarray Facility at the Wellcome Trust Sanger Institute. Bioconductor was used to complete pair comparison analyses of genes differentially expressed at 2 hours and 4 hours infection versus uninfected esDC. At 2 hours infection 3615 genes were differentially expressed with p-value <0.01, of these 1465 genes had p-value <0.001, of which 376 genes had p-value <0.0001. Of the latter class, 325 had a > 2 fold difference in expression, 101 had > 4 fold fold change (of which only one gene was down-regulated), and 8 genes showed and increase in expression higher than 5 and they all were positively activated. Tables of these gene lists can be found in the attached CD. Since there was a high number of gene reported by Bioconductor analysis a further analysis was performed using Innate DB for immune pathway representation. All the corresponding human orthologs were uploaded with the respective p-value and fold change and the results for enrichment in pathway over-representation through InnateDB is reported in Table 6.2 and 6.3.

Table 6.2 InnateDB analysis of genes differentially expressed by esDCs at 2h infection with *S.* Typhimurium SL1344(p1C/1); pathways up-regulated

All the mouse genes with an Ensemble number were further analyzed with InnateDB for pathways. The corresponding human orthologs were determined and the results were enriched using the 'over-representation analysis' option which allows selection of genes on the basis of their fold change (+/- 1.5) and p-value (0.05). The default settings for the analysis algorithm (Hypergeometric) and the multiple testing correction method (The Benjamin & Hochberg correction for the FDR) were used. Only pathways that are significantly up-regulated with p-value < 0.1 are reported here.

Pathway Name of up-regulated pathways at 2h infection	Source Name	Pathway uploaded gene count	Pathway up-regulated genes count	Pathway up-regulated p-value (corrected)
Cytokine-cytokine receptor interaction	KEGG	104	25	0.000930
MAPK signaling pathway	KEGG	171	29	0.059145
Jak-STAT signaling pathway	KEGG	80	17	0.062079
IL12-mediated signaling events	PID NCI	36	11	0.068245
Hematopoietic cell lineage	KEGG	33	10	0.076410

Table 6.3 InnateDB analysis of genes differentially expressed by esDCs at 2h infection with *S.* Typhimurium SL1344(p1C/1); pathways down-regulated

This table reports the pathways down-regulated in esDCs at 2h infection. No down-regulated pathway reported 'corrected p-value' lower than 0.1. For this reason only the top 5 down-regulated pathways with their respective 'non-corrected' p-values are reported here.

Pathway Name of down-regulated pathways at 2h infection	Source Name	Pathway uploaded gene count	Pathway down-regulated genes count	Pathway down-regulated p-value
Valine, leucine and isoleucine degradation	KEGG	28	10	0.000441
Rho GTPase cycle	REACTOME	72	17	0.001369
Vitamin B5 (pantothenate) metabolism	REACTOME	6	4	0.001725
Beta-Alanine metabolism	KEGG	10	5	0.002342
Propanoate metabolism	KEGG	20	7	0.003731

The analysis of genes differentially expressed at 4 hours infection in comparison to uninfected esDC reported 4040 genes with p-value <0.01, of which 1881 had p-value <0.001 including 619 with p-value <0.0001. Of these genes 525 had a fold change in expression > 2, 175 had a fold change in expression > 4 and 117 had a fold change in expression > 5. Due to the large number of genes identified, pathway analysis was used to evaluate the data. Pathways analysis was carried out using InnateDB [www.innatedb.ca] (Lynn *et al.*, 2008) using all the genes resulting from the Bioconductor analysis with the respective p-value and fold change. In this analysis human orthologs were used since InnateDB report a high number of curated interactions in *homo sapiens*. The analysis reported several pathways that were significantly up or down-regulated. The results of this analysis are reported in Tables 6.4 and 6.5.

Table 6.4 InnateDB analysis of genes differentially expressed by esDCs at 4h infection with *S.* Typhimurium SL1344(p1C/1); pathways up-regulated

The expression data obtained from Bioconductor analysis were further analyzed here pathway enrichment using InnateDB. The human orthologs of all genes were uploaded into the browser with the corresponding fold change and p-value. A first pathway analysis was carried out and then an 'over-representation analysis' was conducted using a fold change cut-off of 1.5 and expression p-value 0.05 using the default settings for the analysis algorithm (Hypergeometric) and the multiple testing correction method (The Benjamin & Hochberg correction for the FDR). Only those pathways with adjusted p-values lower then 0.05 are reported here.

GO term Name of pathways up-regulated at 4 hours infection	Source Name	GO term uploaded gene count	GO term up-regulated genes count	GO term up-regulated p-value (corrected)
Cytokine-cytokine receptor interaction	KEGG	104	26	0.000495
IL4-mediated signaling events	PID NCI	33	12	0.004275
IL23-mediated signaling events	PID NCI	24	10	0.004445
Jak-STAT signaling pathway	KEGG	80	20	0.005834
CDK-mediated phosphorylation and removal of Cdc6	REACTOME	36	11	0.019010
IL12-mediated signaling events	PID NCI	36	11	0.019010
Ubiquitin-dependent degradation of Cyclin D1	REACTOME	36	11	0.019010
Ubiquitin Mediated Degradation of Phosphorylated Cdc25A	REACTOME	35	11	0.020413
Vif-mediated degradation of APOBEC3G	REACTOME	35	11	0.020413
Vpu mediated degradation of CD4	REACTOME	34	11	0.021213
Gene expression of SOCS by STAT dimer	INOH	12	6	0.028337
Beta-catenin phosphorylation cascade	REACTOME	39	11	0.032173
Degradation of beta-catenin by the destruction complex	REACTOME	39	11	0.032173
CDT1 association with the CDC6:ORC:origin complex	REACTOME	41	11	0.039599
DNA Replication	REACTOME	41	11	0.039599
Synthesis of DNA	REACTOME	41	11	0.039599
EPO signaling pathway(JAK2 STAT1 STAT3 STAT5)	INOH	9	5	0.041590
Association of licensing factors with the pre-replicative complex	REACTOME	42	11	0.046824

Table 6.5 InnateDB pathway analysis of genes differentially expressed by esDCs at 4h infection with *S.* Typhimurium SL1344(p1C/1); pathways down-regulated

The same gene list analyzed for up-regulated pathways also reported significantly down-regulated pathways. The same parameters were used. This table shows those down-regulated pathways with corrected p-values < 0.05.

GO term Name of pathways down-regulated at 4 hours infection	Source Name	GO term uploaded gene count	GO term down-regulated genes count	GO term down-regulated p-value (corrected)
Citric acid cycle (TCA cycle)	REACTOME	103	26	0.008018
Cori Cycle (interconversion of glucose and lactate)	REACTOME	101	26	0.008018
Glucose metabolism	REACTOME	28	26	0.008018
Oxidative decarboxylation of alpha-ketoglutarate to succinyl CoA by alpha-ketoglutarate dehydrogenase	REACTOME	100	26	0.008018
Pyruvate metabolism and TCA cycle	REACTOME	96	26	0.008018
ChREBP activates metabolic gene expression	REACTOME	101	29	0.008137
Integration of energy metabolism	REACTOME	97	29	0.008137
PP2A-mediated dephosphorylation of key metabolic factors	REACTOME	103	29	0.008137
Electron Transport Chain	REACTOME	94	27	0.008420
Lysine catabolism	REACTOME	95	27	0.008420
Oxidative decarboxylation of pyruvate to acetyl CoA by pyruvate dehydrogenase	REACTOME	95	27	0.008420
Propionyl-CoA catabolism	REACTOME	95	27	0.008420
Regulation of pyruvate dehydrogenase complex (PDC)	REACTOME	95	27	0.008420
Insulin effects increased synthesis of Xylulose-5-Phosphate	REACTOME	95	29	0.008645
Oxidative decarboxylation of alpha-keto-beta-methylvalerate to alpha-methylbutyryl-CoA by branched-chain alpha-ketoacid dehydrogenase	REACTOME	106	29	0.008740
Gamma-Hexachlorocyclohexane degradation	KEGG	106	7	0.008914
Phosphoenolpyruvate and ADP react to form pyruvate and ATP	REACTOME	106	28	0.009170
Oxidative decarboxylation of alpha-ketoisovalerate to isobutyryl-CoA by branched-chain alpha-ketoacid dehydrogenase	REACTOME	92	30	0.009263
Isoleucine catabolism	REACTOME	92	29	0.009771
Mitochondrial fatty acid beta-oxidation of unsaturated fatty acids	REACTOME	92	31	0.009828
Beta oxidation of decanoyl-CoA to octanoyl-CoA-CoA	REACTOME	92	23	0.010158
Beta oxidation of octanoyl-CoA to hexanoyl-CoA	REACTOME	92	23	0.010158
Transcriptional activation of glucose metabolism genes by ChREBP:MLX	REACTOME	108	28	0.010431
Valine, leucine and isoleucine degradation	KEGG	11	13	0.010588
Valine catabolism	REACTOME	79	29	0.010676
Oxidative decarboxylation of alpha-ketoadipate to glutaryl CoA by alpha-ketoglutarate dehydrogenase	REACTOME	79	27	0.010708
Beta oxidation of lauroyl-CoA to decanoyl-CoA-CoA	REACTOME	80	23	0.011196
Beta oxidation of myristoyl-CoA to lauroyl-CoA	REACTOME	80	23	0.011196
Beta oxidation of palmitoyl-CoA to myristoyl-CoA	REACTOME	80	23	0.011196
Beta oxidation of butanoyl-CoA to acetyl-CoA	REACTOME	87	22	0.015703
Oxidative phosphorylation	KEGG	77	24	0.015859
Beta oxidation of hexanoyl-CoA to butanoyl-CoA	REACTOME	78	22	0.018565
Mets affect on macrophage differentiation	PID BIOCARTA	13	7	0.025547

Limonene and pinene degradation	KEGG	13	7	0.025547
Fructose catabolism	REACTOME	7	33	0.027501
Bisphenol A degradation	KEGG	140	5	0.027860
Alanine metabolism	REACTOME	135	32	0.028981
Pentose phosphate pathway (hexose monophosphate shunt)	REACTOME	137	32	0.036902
Dihydroxyacetone phosphate is isomerized to form glyceraldehyde-3-phosphate	REACTOME	139	32	0.045444
Glycolysis	REACTOME	139	32	0.045444

The analysis for pair comparison of esDC expression profile at 4 hours versus 2 hours infection using Bioconductor revealed a few genes differentially expressed. This analysis reported 88 genes differentially expressed with p-value <0.01, and no genes with p-value < 0.001. Pathway analysis was conducted on this gene set using InnateDB as previously described. The 'over-represented analysis' identified one pathway significantly down-regulated at 4 hours compared to 2 hours post-infection, and no up-regulated pathways (Table 6.6).

Table 6.6 InnateDB analysis of genes differentially expressed by esDCs at 4h versus 2h infection with *S.* Typhimurium SL1344(p1C/1); pathway down-regulated

The genes differentially expressed at 4h infection versus 2h infection with *S.* Typhimurium SL1344(p1C/1) were analyzed by InnateDB software to identify pathways significantly up- or down-regulated. The analysis was conducted using human orthologs and the 'over-representation analysis' was conducted using fold change +/- 1.5, p-value <0.1, default settings for the analysis algorithm (Hypergeometric) and the multiple testing correction method (The Benjamin & Hochberg correction for the FDR). No up-regulated pathways were reported and only one down-regulated pathway was revealed as statistically significant.

Name of Pathway down-regulated at 4 hours vs. 2h infection	Source Name	Pathway uploaded gene count	Pathway down-regulated genes count	Pathway down-regulated p-value (corrected)
Arachidonic acid metabolism	KEGG	22	6	0.006221

6.3.6 Real time RT-PCR data on genes differentially expressed by esDCs during infection

Some of the more interesting highly up- or down-regulated genes were chosen for confirmation of the expression results obtained from Bioconductor analysis. For this experiment were selected genes that are involved in ubiquitinylation, Osl1, genes involved in lipid methabolism, Ch25h and Lypla3, components of MHC class I and II, H2-T9 and H2Dma, secreted C-X-C chemokine and interleukine and LPS-inducible kinase localized in the mitocondria. All these genes express proteins probably involved in the immune response and cellular response to the pathogen invasion also a list of functions in which each gene is involved can be found in Table 6.7. The cDNA synthesis was conducted using QIAGEN QuantiTect Reverse Transcription kits. Quantitative RT-PCR was conducted on a STRATAGENE Mx3000P machine using SensiMix Plus SYBR Kit (Quantace) and S18 was employed as an internal control gene. The primers were tested for dissociation products and for efficiency slope before being utilized. The data obtained were analysed using the ΔΔCT method (Livak & Schmittgen, 2001) and the graphical representation of the RT-PCR results is reported in Figure 6.4.

Table 6.7 List of genes chosen to be tested at the RT-PCR to confirm microarray data expression analysis are reported in this table

GeneSymbol	Name	FC	adj.P.Val	GO description
Oasl1	2'-5' oligoadenylate synthetase-like 1	64.00	0.000002	transferase activity // nucleotidyltransferase activity
Tyki	thymidylate kinase family LPS-inducible member	56.49	0.000002	thymidylate kinase activity // ATP binding // dTDP biosynthesis // dTTP biosynthesis
Ch25h	Cholesterol 25-hydroxylase	24.93	0.000021	cellular_component unknown // integral to membrane // steroid hydroxylase activity // oxidoreductase activity // cholesterol metabolism // metabolism
Il6	interleukin 6	8.34	0.000090	extracellular // extracellular space // growth factor activity // cytokine activity // interleukin-6 receptor binding // immune response // acute-phase response
H2-T9	histocompatibility 2, T region locus 9	5.90	0.000062	integral to membrane // defense response
Cxcr4	chemokine (C-X-C motif) receptor 4	-2.83	0.004630	integral to membrane // G-protein coupled receptor activity // chemokine receptor activity // rhodopsin-like receptor activity // C-X-C chemokine receptor activity // T-cell proliferation // defense response // brain development // chemotaxis // regulation of cell migration
H2-Dma	histocompatibility 2, class II, locus Mb1	-3.89	0.001420	integral to membrane // extracellular space // MHC class II receptor activity // defense response //immune response // antigen processing, exogenous antigen via MHC class II
Lypla3	lysophospholipase 3	-11.08	0.000019	soluble fraction // lysophospholipase activity // calcium-independent cytosolic phospholipase A2 activity // calcium-independent phospholipase A2 activity // ceramide metabolism

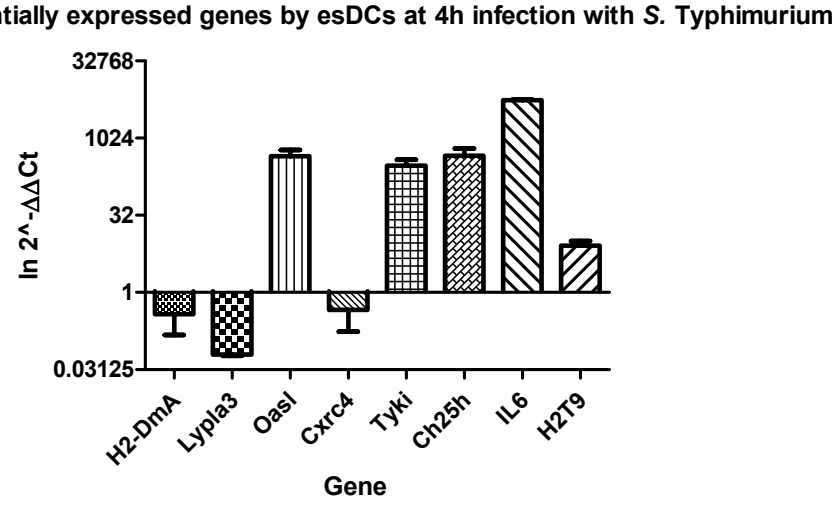

Figure 6.4 Graphical representation of qRT-PCR results

The Ct values obtained from three technical replicates for each biological replicate were analyzed using the delta-delta method and reported as the $Ln2^{\wedge -\Delta\Delta Ct}$ values. These data confirm the Bioconductor analysis of up- or down-regulated genes.

6.3.7 Statistical analysis of the RT-PCR data on genes differentially expressed by esDCs during infection

The RT-PCR data were statistically analyzed using REST© software, designed to analyse relative quantitation in qRT-PCR to determine whether there is a significant difference between samples and control, while taking into account reaction efficiency and reference gene normalization. It applies a simple statistical randomization test (Herrmann & Pfaffl, 2005). The results of this analysis are reported in Figure 6.5 and in Table 6.8.

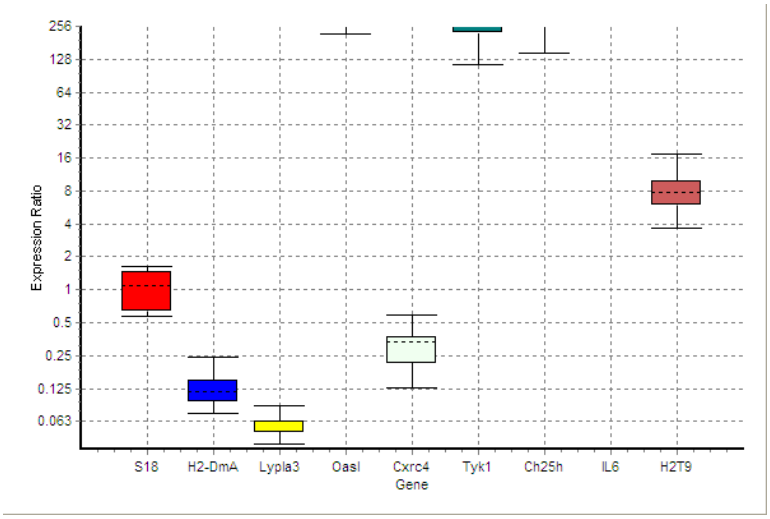

Figure 6.5 Whisker-Box plots for RT-PCR results statistical analysis

The RT-PCR Ct values obtained from three technical replicates for each biological replicate, to test the expression of eight genes, were statistically analysed with REST-2005. This graph reports the skew of distribution of the values reporting the sample median (dotted line), box represents 50% of all observations, and the whiskers represent outer 50% of all observations.

Table 6.8 Summary of the statistical analysis on Ct values obtained from qRT-PCR analysed with REST-2005

Gene	Type	Reaction Efficiency	Expression	Std. Error	P(H1)	Result
H2-DmA	TRG	1	0.041	0.029 - 0.056	0.031	DOWN
Lypla3	TRG	1	0.019	0.016 - 0.026	0.032	DOWN
Oasl	TRG	1	127.803	78.835 - 185.476	0	UP
Cxrc4	TRG	1	0.095	0.052 - 0.155	0.016	DOWN
Tyk1	TRG	1	96.838	56.722 - 193.327	0	UP
Ch25h	TRG	1	128.494	69.293 - 222.202	0	UP
IL6	TRG	1	1,574.37	1,136.096 - 2,555.907	0	UP
H2T9	TRG	1	2.569	1.671 - 4.027	0.068	

The target genes' Ct values were analyzed for statistical significant difference compared to the internal control gene S18's Ct value. All the genes were confined to be significantly differentially expressed with p-value < 0.07. These results confirmed the Bioconductor analysis performed on esDC expression during *S.* Typhimurium infection.

6.4 Discussion

The ability of microarray analysis to detect expression patterns across the entire genome permits an investigation of a large number of genes in a few experiments. Since tens of thousands of genes are investigated the number of genes differentially expressed and transcripts involved in the same biological function can be identified. However, the data interpretation of the data can be challenging. In this study thousands of genes were revealed as up- or down-regulated in esDCs during infection with *S.* Typhimurium SL1344(p1C/1), and although it was possible to recognize some genes with known involvement in host-pathogen interactions, pathway analysis was uded to provide a further insights into host-pathogen interaction. For this reason transcription results obtained in this study on esDCs infected with *S.* Typhimurium were as analyzed to identify pathways that were up- or down–regulated during infection. Below is a discussion of some of the pathways revealed in this study and their possible role in *Salmonella* invasion.

The pathways significantly up- or down-regulated at 2 hours and at 4 hours post-infection are reported in Table 6.2, 6.3 6.4 and 6.5. After 2 hours infection five pathways were significantly up-regulated: 'cytokine-cytokine receptor interaction', 'Jak-STAT signaling pathway' and 'IL-12 mediated signaling events' (these were also up-regulated at 4 hours), and the 'hematopoietic cell lineage' and 'MAPK signaling pathway' (which were up-regulated only at 2 hours).

It is important to note that the 'IL-12 mediated signaling events' was up-regulated both at 2 hours and at 4 hours infection. The production of IL-12 is a specific signature of APCs and although IL-12 subunits themselves weren't identified as up-regulated in the Bioconductor analysis, the pathway analysis reveals that probably at the 4 hours post-infection, time of analysis, this pathway was not expressed completely as can be seen in Figure 6.6 where the final products of the pathway are not reported. Previous studies highlighted a predominant expression of IL-12p40 during *Salmonella* infection (Johansson & Wick, 2004). However other studies demonstrated that *Salmonella* infection of BMDC induce stronger production of p40, IL-12, IL-23 and IL-27p28 than bone marrow-derived macrophages (Siegemund *et al.*, 2007). IL-12, a heterodimeric

cytokine composed by two subunits p35 and p40 covalently linked, is part of a family of cytokine comprising IL-12, IL-23, IL27 and IL12p40. The subunit p35 is produced in small amounts whereas the subunit p40 is produced in surplus. Homodimeric p40 can act as an IL-12 antagonist for its receptor and can bind to another protein p19, related to p35, and form another cytokine IL-23. Interestingly, the 'IL-23-mediated signaling events' pathway was also up-regulated at 4 hours post-infection, Table 6.4. IL-12 is involved in the induction of cell-mediated immunity to intracellular pathogens by promoting the differentiation of the Th1 cellular response via IFNγ production from T cells and NK cells. IL-12 is essential for the ability of the host to fight against intracellular bacteria and its lack results in immunodeficiency and induce susceptibility to infections (de Jong *et al.*, 1998; Magram *et al.*, 1996a; Magram *et al.*, 1996b; Mattner *et al.*, 1996). The activities of IL-12 are mediated by a high affinity receptor formed by two subunits β1 and β2, which are members of the class I cytokine receptor family and are most closely related to glycoprotein gp130. Binding to the receptor subunit β1 induce a chain reaction involving the biding of STAT4 (signal transducer and activator of transcription 4) supporting the data that STAT pathways were also up-regulated.

Bioconductor analysis revealed the expression of two IL-12 receptors in esDCs at 4 hours infection with *S.* Typhimurium, IL-12R was down regulated slightly (-1.1 fold) with a p-value of 0.0793 and IL-12Rβ2 was not significantly up- or down-regulated (1 fold with a p-value 0.785). Figure 6.6 shows the IL-12 mediated pathway.

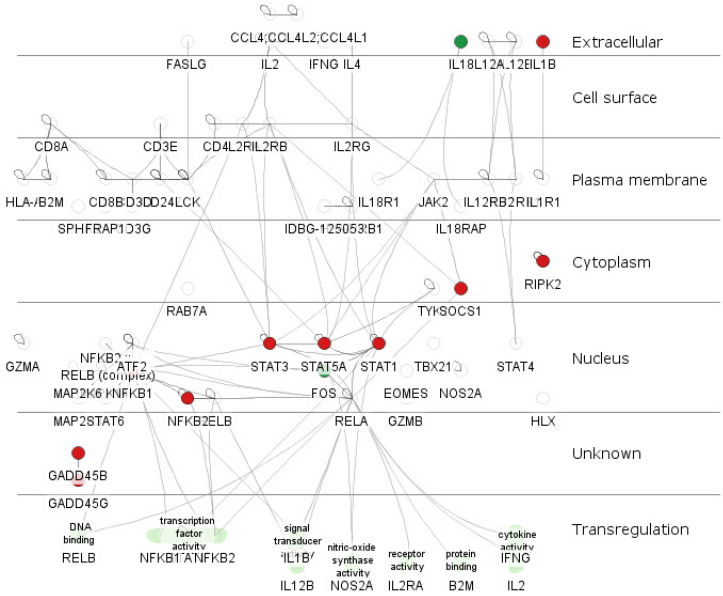

Figure 6.6 This Cytoscape picture represents the IL-12-mediated pathway at 4h

In red are the genes up-regulated and in green the genes down-regulated as result of the Bioconductor analysis.

One other interesting pathway up-regulated by esDCs during infection with *S.* Typhimurium is the 'IL-4-mediated signaling events'. IL-4, together with IL-10, forms part of an anti-inflammatory pathway. IL-4 is an important cytokine since it is involved in the maturation of naïve T cells into Th2 cells. Interestingly, it is still not clear which type of cell produces this cytokine *in vivo*. A recent study has shown how basophils have the ability to produce IL-4 cytokine in response to a model protease allergen, papain, following recruitment into the lymph node (Sokol *et al.*, 2008). However, production of IL-4 from DCs during *C. albicans* hyphae infection but not during the yeast phagocytosis has also been described. The researchers advanced the hypothesis that DCs are capable of discriminating between the two forms of the fungus (d'Ostiani *et al.*, 2000). In the Bioconductor pair comparison analysis IL-4 was found to be up-regulated 2.6 fold (p-value 0.0743) in esDCs at 4 hours after infection with *S.* Typhimurium SL1344.

Furthermore, the data indicated that suppressor cytokine signaling (SOCS) genes 1 and 3 were up-regulated and that SOCS2 was down-regulated. This pathway is probably connected to the 'Cytokine-cytokine receptor interaction', the 'Jak-STAT signaling pathway' and the 'EPO signaling pathway'. SOCS genes encode a family of 7 proteins

which act as negative regulators of the JAK/STAT signaling pathway usually activated in response to cytokine and hormones. The phosphorylation of STAT by JAK is necessary for dimerization, nuclear transportation, DNA binding and gene transcription (Yasukawa *et al.*, 2000). Alteration in the expression of these genes during *Salmonella* infection has been described previously. Uchiya and Nikai (2005) reported that SOCS 1 and 3 expression is regulated by SPI-2 products. In addition, it was previously reported that SpiC protein, expressed from SPI-2, is able to inhibit the lysosomal fusion with the SCV (Uchiya *et al.*, 1999). Other published work has shown that this protein is traslocated in the host cell cytoplasm through the TIIISS encoded on SPI-2 and that it is able to interact with the host proteins TassC (Lee *et al.*, 2002) and Hook3 (Shotland *et al.*, 2003), involved in cellular trafficking. SpiC appears to play a central role in the pathogen intracellular survival (Freeman *et al.*, 2002; Yu *et al.*, 2004). The enhanced expression of SOCS3 in macrophages during *Salmonella* infection is driven by the SpiC protein. Finally, SOCS3 inhibits cytokine signaling by blocking the phosphorylation of STAT-1 or STAT-3, inducing respectively the inhibition of IL-6 and IFNγ secretion (Uchiya & Nikai, 2005). Figure 6.8 shows the SOCS pathway with up- and down-regulated genes identified by Bioconductor analysis.

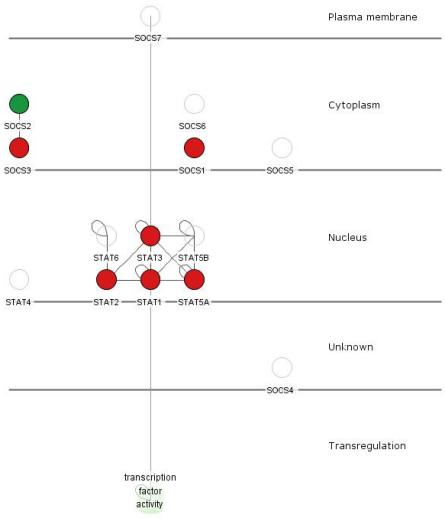

Figure 6.7 Cytoscape representation of the SOCS pathway in esDCs at 4h infection

The red genes were up-regulated and the green genes were down-regulated in the pair comparison analysis at 4h infection performed with Bioconductor.

Among the down-regulated pathways, there are many oxidative pathways involving acetyl-CoA and most of the down-regulated pathways take place in the mitochondrion. Unfortunately these pathways are not as well annotated as are the up-regulated pathways. It can be quite challenging in this situation to advance a hypothesis and speculate on what really happens during infection. However a comparison with the literature can help; for example it was reported early in 2008 that *S.* Typhimurium SR-11 carrying mutations in the tricarboxylic acid (TCA) cycle and unable to convert succinate to fumarate, are attenuated, whereas mutants that were not able to run a reductive branch of the TCA were fully virulent (Mercado-Lubo *et al.*, 2008). It can be speculated that these mutant bacteria use the host cells apparatus, and in this situation the host cell attempts to down-regulate its own TCA in order make components less available to the bacteria.

On the other hand, the mitochondria are important organelles involved in the regulation of many different pathways including the KREB cycle, heme synthesis, ATP and NADPH synthesis. The general down-regulation of the oxidative pathways could affect heme synthesis. Although the heme synthesis pathway was not differentially expressed in the analysis reported here. Heme synthesis relies on the mitochondrion and the cytosol and involves succinyl-CoA and glycine. Heme is synthesized in all human nucleated cells at different rates. Accumulation of intracellular or extracellular heme can be harmful to cells and free heme mediates oxidative stress and inflammation. Heme can affect a wide range of regulatory factors and can influence gene expression at almost every level regulating transcription (Zhang & Guarente, 1995), mRNA stability (Maniatis *et al.*, 1976), protein synstesis (via eIF-2αkinase, that was up-regulated during murine ES cells infection) (Chen *et al.*, 1994), splicing (Ponka, 1999), and post-translational modifications (Swenson *et al.*, 1991). Heme also induces nitric oxide synthesis and regulated Cytocrome P450 expression (Wagener *et al.*, 2003). A strong down-regulation of P450 was observed during ES cells infection. It is possible that the infected cells try to starve the pathogen for iron supply. In fact it has been shown previously that bacteria require iron to survive inside the host cell and for this reason they have evolved mechanisms that permit them to acquire iron from mammalian iron carriers: transferrin and heme, in addition to the production of low-molecular weight molecules with high affinity for Fe^{3+} denominated siderophores (Milne *et al.*, 2007).

In conclusion, in this chapter are reported the results of a transcriptome analysis of esDCs during *S.* Typhimurium infection. As in all of this type of work, the whole microarray analysis cannot possibly give any kind of specific answer but gives ideas and direction for future research and this report is a good example of its type.